# Measuring the impact of Ebola control measures in Sierra Leone

Adam J. Kucharski[1], Anton Camacho, Stefan Flasche, Rebecca E. Glover, W. John Edmunds, and Sebastian Funk

Centre for the Mathematical Modelling of Infectious Diseases, Department of Infectious Disease Epidemiology, London School of Hygiene & Tropical Medicine, London WC1E 7HT, United Kingdom

Edited by Burton H. Singer, University of Florida, Gainesville, FL, and approved September 10, 2015 (received for review May 5, 2015)

**Between September 2014 and February 2015, the number of Ebola virus disease (EVD) cases reported in Sierra Leone declined in many districts. During this period, a major international response was put in place, with thousands of treatment beds introduced alongside other infection control measures. However, assessing the impact of the response is challenging, as several factors could have influenced the decline in infections, including behavior changes and other community interventions. We developed a mathematical model of EVD transmission, and measured how transmission changed over time in the 12 districts of Sierra Leone with sustained transmission between June 2014 and February 2015. We used the model to estimate how many cases were averted as a result of the introduction of additional treatment beds in each area. Examining epidemic dynamics at the district level, we estimated that 56,600 (95% credible interval: 48,300–84,500) Ebola cases (both reported and unreported) were averted in Sierra Leone up to February 2, 2015 as a direct result of additional treatment beds being introduced. We also found that if beds had been introduced 1 month earlier, a further 12,500 cases could have been averted. Our results suggest the unprecedented local and international response led to a substantial decline in EVD transmission during 2014–2015. In particular, the introduction of beds had a direct impact on reducing EVD cases in Sierra Leone, although the effect varied considerably between districts.**

Ebola virus disease | Sierra Leone | control measures | treatment beds | mathematical model

The 2013–2015 Ebola virus disease (EVD) epidemic in West Africa has seen more cases than all past outbreaks combined (1), and has triggered a major international response. In Sierra Leone, where there have been over 8,600 confirmed cases reported as of 2015 August 1, the Sierra Leone and UK governments and nongovernmental organizations have supported the gradual introduction of over 1,500 beds in Ebola Holding Centers (EHCs) and Community Care Centers (CCCs), as well as over 1,200 beds in larger-scale Ebola Treatment Units (ETUs) (2, 3). As well as the humanitarian value of providing treatment and care to sick patients, there is a secondary benefit to expanding bed capacity that is more difficult to quantify; by isolating the ill and removing them from the community, further infections might be prevented.

Since the peak of the epidemic in Sierra Leone in November 2014, when there were over 500 confirmed EVD cases reported per week, the level of infection has dropped, with fewer than 100 confirmed cases reported per week in February 2015. Although the nationwide decline in cases coincided with an increase in the number of beds available (4), as well as improved case detection, tracing of contacts, and safe burials of patients who had died (3, 5), there has been criticism of the timing and focus of the international response in Sierra Leone (6, 7). To properly evaluate the control efforts, and plan for future outbreaks of EVD, it is therefore crucial to understand how many cases were likely averted as a result of the response.

Mathematical models have been used prospectively to estimate the potential impact of additional beds (8–11). However, evaluating the effect of control measures retrospectively is more challenging, because a model must disentangle the reduction in transmission due to improved bed capacity from other factors. Behavior changes (12), community engagement, improved case finding, and an increase in safe burials (5) could all have contributed to a reduction in transmission. Indeed, many Ebola facilities were designed to be part of a package of interventions, combining treatment beds with community-based infection control (3).

To estimate how EVD transmission changed as interventions were introduced, we developed a stochastic mathematical model of Ebola transmission in Sierra Leone. The model was stratified by district, and incorporated available data on bed capacity in ETUs, EHCs, and CCCs (13). As beds were not the only control measure in place, we also included a time-varying transmission rate in the model (4, 14) to capture any variation in transmission which was not explained by the introduction of beds.

As not all new cases in Sierra Leone occurred among known contacts of EVD patients (15), we accounted for potential underreporting in our model. In our main analysis, we assumed that 60% of infectious individuals would be ascertained (i.e., would be reported and seek treatment), and that it took an average of 4.5 d for these individuals to be reported (16). We also included the possibility of variability in the accuracy of reporting, with weekly reported cases following a negative binomial distribution. In the model, stochasticity could therefore be generated by both the transmission process and the reporting process. We assumed infectious individuals who were ascertained attended EHCs/CCCs if beds were available (16); the average time between onset and attendance declined over time, based on reported values for Sierra Leone (*SI Appendix*, Fig. S1). Once test results were received, patients were transferred to an available ETU; we

## Significance

**Between June 2014 and February 2015, thousands of Ebola treatment beds were introduced in Sierra Leone, alongside other infection control measures. However, there has been criticism of the timing and focus of this response, and it remains unclear how much it contributed to curbing the 2014–2015 Ebola epidemic. Using a mathematical model, we estimated how many Ebola virus disease cases the response averted in each district of Sierra Leone. We estimated that 56,600 (95% credible interval: 48,300–84,500) Ebola cases were averted in Sierra Leone as a direct result of additional treatment beds. Moreover, the number of cases averted would have been even greater had beds been available 1 month earlier.**

Author contributions: A.J.K., A.C., W.J.E., and S. Funk designed research; A.J.K. performed research; R.E.G. contributed new reagents/analytic tools; A.J.K., A.C., S. Flasche, W.J.E., and S. Funk analyzed data; R.E.G. performed data extraction and cleaning; and A.J.K., A.C., S. Flasche, W.J.E., and S. Funk wrote the paper.

The authors declare no conflict of interest.

This article is a PNAS Direct Submission.

Freely available online through the PNAS open access option.

[1]To whom correspondence should be addressed. Email: adam.kucharski@lshtm.ac.uk.

This article contains supporting information online at www.pnas.org/lookup/suppl/doi:10.1073/pnas.1508814112/-/DCSupplemental.

assumed this took 2 d on average. If no beds were available at any facility, cases remained in the community. The model structure is shown in Fig. 1, and the full set of parameter values in *SI Appendix*, Table S1.

To allow for a time-varying community transmission rate, we used a flexible sigmoid function (14, 17); depending on parameter values, transmission could be constant over time, or increase or decline. Our model structure therefore made it possible to separate the reduction in infection as a result of additional treatment beds and variation resulting from other effects, such as behavior changes and implementation of safe burials.

We used a Bayesian approach to fit the model to weekly EVD confirmed and probable case data reported in each district of Sierra Leone (18, 19), and to estimate how community transmission varied over time. We then used the fitted model to simulate multiple stochastic epidemic trajectories, and measured the number of cases that could have occurred in each district had additional beds not been introduced.

## Results

We found that the temporal change in community transmission varied considerably between different regions (Fig. 2). In Bo and Moyamba, for example, the level of community transmission remained relatively flat, whereas in Bombali, Kailahun, Port Loko, and Western Area, a significant decline in community transmission occurred alongside the reduction in transmission resulting from additional beds. In districts where there was greater variation in disease incidence, such as Kambia and Kenema, there was considerable uncertainty in our estimates of the community transmission rate. We found that the decline in community transmission in each of the 12 districts was strongly associated with the initial basic reproduction number, but less so with the total number of cases (*SI Appendix*, Table S2). There was also a geographical structure to the decline, with a greater drop occurring in districts in the north and east of the country (*SI Appendix*, Fig. S2).

To measure how many cases control measures may have averted, we removed all CCC, EHC, and ETU beds introduced during the period of observation and simulated stochastic epidemic trajectories using our estimates for the time-varying level of community transmission (*SI Appendix*, Fig. S3). In this scenario, transmission reductions from factors other than beds, such as reduced infection as a result of behavior changes, were still included. Any difference in epidemic dynamics between this scenario and the original model was therefore only the result of the removal of treatment beds.

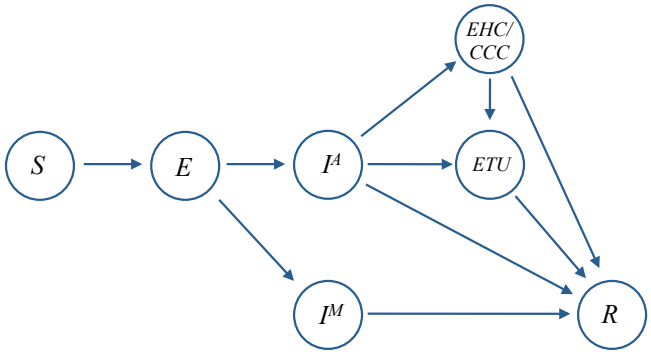


**Fig. 1.** Model structure. Individuals start off susceptible to infection (*S*). Upon infection with Ebola they enter an incubation period (*E*), then at symptom onset they become infectious; these individuals either eventually become ascertained ($I^A$) or do not ($I^M$). Individuals who are ascertained initially seek health care in EHCs/CCCs (or ETUs if these are full); if no beds are available, they remain infectious in the community until the infection is resolved (*R*), i.e., they have recovered, or are dead and buried. Patients in EHC/CCCs are transferred to ETUs once they have been tested for Ebola, which takes an average of 2 d. Patients remain in ETUs until the infection is resolved. We assume the latent period is 9.4 d, the average time from onset to EHC/CCC attendance declines from an initial value of 4.6 d (*SI Appendix*, Fig. S1), and individuals who do not seek treatment are infectious for 10.9 d on average (details in *SI Appendix*).

Our results suggest that the increase in beds averted a limited number of cases in districts without ongoing transmission (e.g., Pujehun) but in districts with large outbreaks—such as Bombali and Western Area—there would have been thousands more infections without the introduction of beds. In Kenema, which had highly variable incidence data, there was substantial variation in the background transmission rate, and hence it was not possible to detect a significant effect of interventions; the 95% credible interval (CI) for cases averted includes zero in Table 1. Across all 12 districts, we estimated that 56,600 (95% CI: 48,300–84,500) cases were averted in total between June 2014 and February 2015 as a result of additional beds.

As a sensitivity analysis, we also estimated how many cases would have been averted if 40% or 80% of cases were ascertained, rather than 60% as in our main analysis (*SI Appendix*, Tables S3 and S4). If 80% of cases were ascertained, we estimated that 148,000 (95% CI: 115,000–219,000) cases were potentially averted across all districts as a result of the introduction of beds; when ascertainment was 40%, the additional beds averted 29,200 (95% CI: 24,500–47,700) cases. In our main analysis, we also assumed an infectious period of 10.9 d, based on reported time from onset-to-death, and onset-to-hospital discharge (details in *SI Appendix*). As some cases may have ceased to be infectious before discharge, as a sensitivity analysis we refit the model with a 9-d infectious period, equal to the average time of infectiousness for fatal cases. Our results did not change substantially under this assumption (*SI Appendix*, Table S5).

In the model, we also assumed that transmission in each district was independent of the others. In reality, however, infectious individuals occasionally traveled between different areas (20). To assess how this could affect our estimates of cases averted, we resimulated outbreaks using the fitted model, but with additional infectious individuals introduced at a rate of either one per day or one per week in each district. When there was an average of one additional infection introduced per week, our estimates increased slightly (*SI Appendix*, Table S6); when one additional infection was introduced per day, the increase was larger, with an estimated 72,900 (95% CI: 61,700–87,900) cases averted across the country.

As well as measuring the effect of actual control measures, we were also able to estimate what impact the introduction of beds would have had earlier in the epidemic. Using the fitted model, we simulated epidemic trajectories under the assumption that the same numbers of beds were introduced 4 wk earlier than in reality (*SI Appendix*, Fig. S4). In this scenario, we estimated 69,100 (95% CI: 59,500–122,000) cases would have been averted, which is 12,500 higher than the number we estimated were actually averted (Table 1).

## Discussion

Using a district-level mathematical model of EVD transmission, we have examined the effect of control measures on epidemic dynamics in Sierra Leone. In particular, we estimated the effect of the reduction in community transmission and additional treatment beds on the number of EVD cases. We found considerable geographic variation: in some districts, there was a noticeable shift in epidemic dynamics as a result of changes in community transmission and increased bed capacity; in other areas, the impact of control measures was less clear.

Although we could measure the number of beds available over time, there were some additional components of the treatment process that were less well known. We used reported data on time to hospital admission in Sierra Leone to parameterize our model

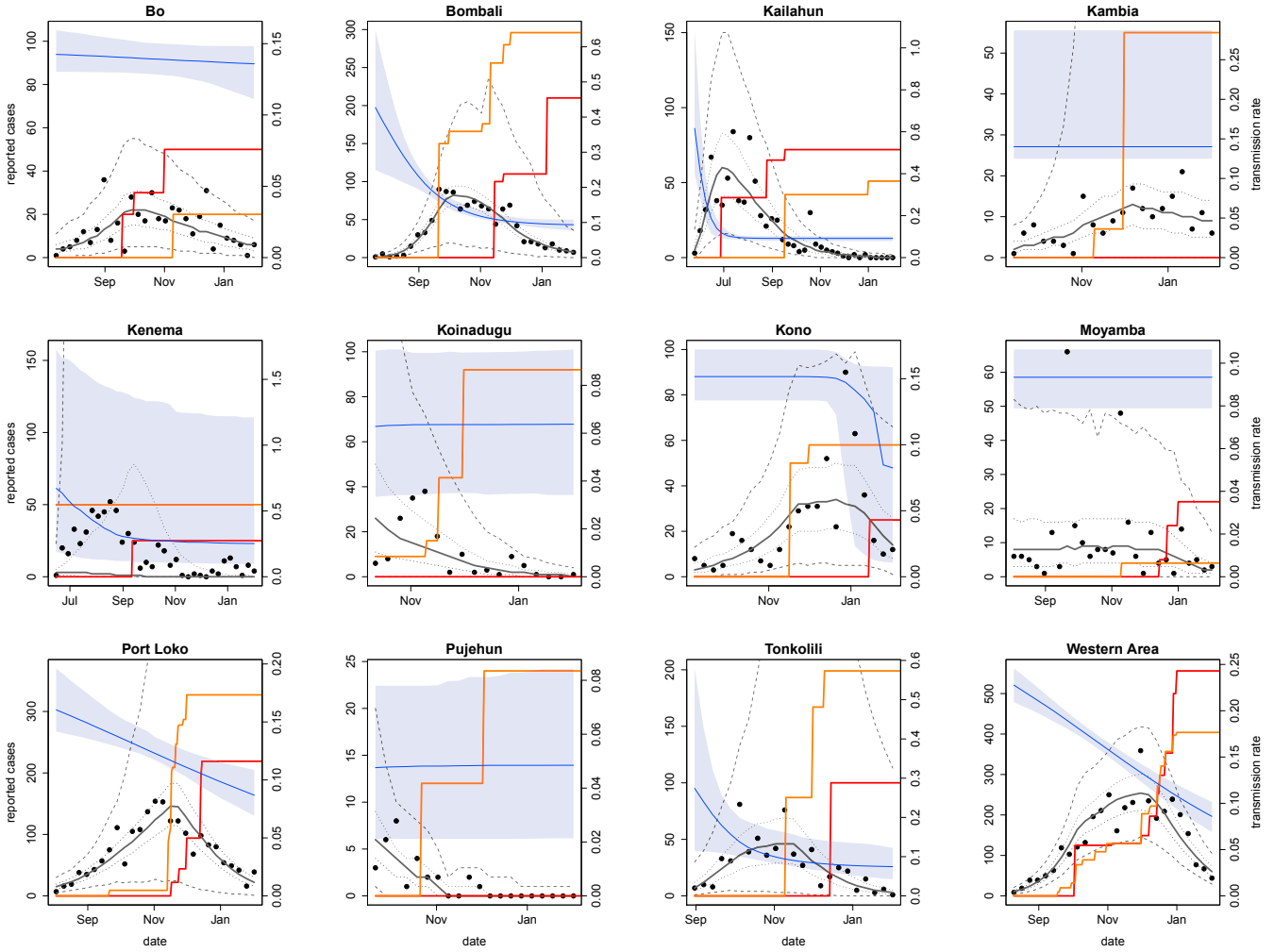


**Fig. 2.** Community transmission and bed capacity in Sierra Leone over time. Blue lines show estimated median community transmission rate, shaded area shows 95% CI (right-hand axis). Black dots show weekly reported confirmed and probable cases in each district up to February 2, 2015 (left-hand axis). Gray lines show median number of cases generated from 1,000 simulations of the fitted model, with 50% CI given by dotted gray lines and 95% CI given by dashed lines. Solid red lines, ETU bed capacity; orange lines, EHC/CCC bed capacity.

(1, 16), but this may have varied between districts. We also assumed that individual infectiousness remained constant throughout the symptomatic period. If most transmission occurs in the later stages of infection, as viral load data might suggest (21), treatment beds could have had a greater impact on transmission reduction by isolating cases at their most infectious. This would make our estimate for cases averted as a result of additional beds conservative.

In the model, patients also sought treatment within their home district. However, in the early stages of the epidemic, several cases admitted to the ETU in Kailahun were from outside the district (20). This may have increased the benefits of bed introduction, by reducing transmission in locations without treatment beds; it may also have impeded control efforts, by making contact tracing and safe burials more difficult (20). In addition, faster turnaround time in laboratory testing may have reduced the time spent in EHCs/CCCs before moving to ETUs (Sierra Leone Ebola labs project – beating the outbreak at source; https://publichealthmatters.blog.gov.uk/2015/03/18/sierra-leone-ebola-labs-project-beating-the-outbreak-at-source/), and led to more EHC beds becoming available per day. Although there were occasional details of the number of patients in isolation in different districts in Ministry of Health and Sanitation situation reports (15), overall these data were incomplete. If more complete EHC/CCC/ETU data were available, it would be possible to validate our model estimates for the number of cases hospitalized over time.

Our results also emphasize the highly variable nature of Ebola transmission. Even in retrospect, it was difficult to measure the effect of changes in transmission and additional beds on the number of EVD cases in some areas. It is also likely that the introduction of Ebola facilities helped stimulate other infection control measures, including safe burials and improved contact tracing (3). In our simulated scenarios, we removed only treatment beds; in practice, a lack of treatment centers would also likely have led to fewer safe burials, and hindered investigation of cases' contacts. With better data on the timing and role of different interventions—both clinical and nonclinical—it would be possible to obtain more accurate estimates about the precise contribution of different factors to the dynamics of EVD in Sierra Leone. In particular, it is important to understand how awareness of EVD influences behavior during an outbreak (22), and how this change in behavior might affect disease dynamics (23, 24).

In the absence of such data, we concentrated on the impact of additional treatment beds alone; we assumed the level of community transmission declined regardless of the number of beds. An alternative approach would be to assume that transmission would remain at the same level as was in the early phase of the

**Table 1. Estimated number of cases averted up to February 2, 2015 as a result of additional treatment beds**

| District | Initial $R_0$ | Beds introduced | Additional beds | Beds 4 wk earlier |
|---|---|---|---|---|
| Bo | 1.6 (1.4–1.7) | 124 | 6,310 (4,150–9,040) | 6,820 (4,730–9,620) |
| Bombali | 5.2 (2.9–7.9) | 506 | 6,480 (1,800–22,900) | 7,630 (2,320–34,500) |
| Kailahun | 8.4 (5.3–16.2) | 123 | 3,650 (2,250–6,750) | 4,580 (3,290–7,460) |
| Kambia | 1.5 (1.4–3.6) | 55 | 545 (2–4,430) | 748 (4–15,400) |
| Kenema | 7.4 (2.1–19.4) | 75 | 1 (0–10,500) | 3 (0–23,800) |
| Koinadugu | 0.7 (0.3–1.1) | 92 | 35 (11–104) | 97 (48–206) |
| Kono | 1.6 (1.4–1.9) | 83 | 1,570 (928–2,430) | 2,060 (1,490–3,060) |
| Moyamba | 1 (0.9–1.2) | 34 | 130 (77–197) | 237 (145–366) |
| Port Loko | 1.8 (1.6–2.2) | 546 | 3,850 (853–13,400) | 5,660 (1,180–26,900) |
| Pujehun | 0.5 (0.2–1.2) | 24 | 11 (2–34) | 22 (6–55) |
| Tonkolili | 3.5 (1.3–8.4) | 349 | 568 (140–2,900) | 959 (272–5,940) |
| Western Area | 2.5 (2.2–2.8) | 960 | 32,600 (25,500–40,200) | 39,200 (32,100–47,100) |
| Total | | 2,971 | 56,600 (48,300–84,500) | 69,100 (59,500–122,000) |

For each district, we estimated the median number of additional cases that would result in the original fitted model, with community transmission rate varying as shown in Fig. 2. We then considered two scenarios: additional EHC/CCC/ETU beds introduced as in reality, and the same additional beds introduced 4 wk earlier, and estimated the number of cases averted in each scenario (95% CI in parentheses). The median posterior estimates for initial $R_0$ (95% CI in parentheses) and total numbers of additional EHC/CCC/ETU beds introduced in each district are shown for comparison.

epidemic (9, 10). As our estimate of the basic reproduction number $R_0$ was above 1 in most districts initially (Table 1), epidemic theory suggests the outbreak would have continued to grow exponentially in these regions under the assumption of no change in transmission, until there were insufficient susceptible individuals for the infection to persist. The corresponding number of cases averted would therefore have been extremely large. However, it was not clear that $R_0$ would have remained unchanged for such a long period. Evidence from past EVD epidemics indicates that changes in behavior can reduce transmission independently of external interventions (22, 25).

Even under our conservative assumption that the introduction of EHCs/CCCs/ETUs reduced transmission only by isolating more patients, we estimated that around 57,000 cases were averted in Sierra Leone as a result of additional treatment beds. Given that the case fatality rate of Ebola in Sierra Leone is near 70% (16), this suggests that the scale-up of local and international efforts to combat the epidemic is likely to have averted over 40,000 Ebola deaths in the country between June 2014 and February 2015. Moreover, the reduction in Ebola transmission will also have halted the damaging secondary effects of the epidemic, including the suspension of access to maternal health and vaccination programs (26, 27).

## Materials and Methods

**Transmission Model.** To model the effect of treatment beds on Ebola transmission, we used a susceptible-exposed-infectious-removed (SEIR) framework that incorporated ETUs and EHCs/CCCs (8). We used a relatively simple framework as we were fitting to only a single case timeseries for each district (14). In the model, individuals started off susceptible to infection ($S$). Upon infection with Ebola they entered an incubation period ($E$), then at symptom onset they became infectious. As there is evidence that not all Ebola cases have been reported (1), we assumed that only a proportion $r$ of newly infectious individuals would eventually be ascertained and seek treatment. This category was denoted $I^A$. The other proportion $1-r$ would not be ascertained; this group was denoted $I^M$. We assumed that it took an average of $1/\tau_r$ d for ascertained cases to be reported to the Ministry of Health. After becoming symptomatic in the model, cases in $I^A$ sought health care in EHCs/CCCs ($H$). They took an average of $1/\tau_H$ d to attend these centers. If no EHC/CCC beds were available, the patient would attend an ETU. If no ETU bed were available, the patient remained infectious in the community until the infection was resolved ($R$); i.e., they had recovered, or were dead and buried. Once in an EHC/CCC, patients were tested for Ebola (we assumed this took an average of 2 d) then progressed to an ETU if a bed was available. Patients stayed for an average of $1/\tau_D$ d in an ETU before the disease was resolved (either through recovery or death). The probability that Ebola-positive individuals were admitted to an EHC/CCC, $p_H$, when they attended the center depended on whether the center was full or not. We assumed that some patients attending EHCs/CCCs were Ebola-negative, which had the effect of reducing the available bed capacity by a factor $\alpha$. The probability that Ebola-positive individuals were admitted to an EHC/CCC upon attendance was therefore

$$p_H = \begin{cases} 1 & \text{if } \alpha B_H > H \\ 0 & \text{if } \alpha B_H = H' \end{cases} \quad [1]$$

where $B_H$ denotes the total capacity of the EHCs/CCCs. Likewise, the probability that individuals were admitted/transferred to an ETU was

$$p_U = \begin{cases} 1 & \text{if } B_U > U \\ 0 & \text{if } B_U = U' \end{cases} \quad [2]$$

where $B_U$ denotes the capacity of the ETUs. We assumed that the population was initially fully susceptible to infection. We assumed the average latent period $1/\nu$ was 9.4 d, and the average duration of infectiousness in the community $1/\gamma$ to be 10.9 d in our main analysis; as a sensitivity analysis we also considered an infectious period of 9 d. The average time from onset-to-outcome for individuals that seek treatment was assumed to be 11.3 d (details in *SI Appendix*).

We obtained EHC/CCC/ETU opening dates from the Humanitarian Data Exchange (13), and cleaned ambiguous or missing dates using reports from the World Health Organization (WHO), Médecins Sans Frontières, UNICEF, and other partners. If the precise date of opening or change in capacity was not known, we used the first date for which we could find confirmation of the center being open with a given capacity. This could have made our analysis more conservative, as some centers may in reality have opened earlier than we presumed. One field study in Bo estimated that 54% of EVD cases made it into the district-level situation reports (28); in turn, the numbers of cases in these reports are typically slightly lower than the numbers in the final WHO patient database (1). Therefore, we made the assumption that 60% of symptomatic cases were ascertained in our main analysis (4), and considered 40% and 80% ascertainment as a sensitivity analysis. We assumed that it took an average of 4.5 d for these cases to be reported after symptom onset (16) In the model, the time between onset and attendance of EHCs/CCCs declined from 4.6 to 1.3 d between July 2014 and April 2015 (*SI Appendix*, Fig. S1); the average duration spent in EHC/CCC before moving to an ETU was 2 d; and the average time spent in an ETU was initially 11.3 − 4.6 − 2 = 4.7 d. We assumed that 50% of beds in EHCs/CCCs were occupied by Ebola-negative patients (15) (i.e., $\alpha = 0.5$). We also allowed community transmission to potentially vary over time by modeling the transmission rate at time $t$, $\beta_t$, as a sigmoid (14, 17):

$$\beta_t = \hat{\beta}\left(1 - \frac{a_2}{1 + e^{-a_1(t-a_\tau)}}\right), \quad [3]$$

where $\hat{\beta}$, $a_1$, $a_2$, and $a_\tau$ were parameters to be fitted. We modeled transmission dynamics using a stochastic model, with environmental noise acting on the transmission rate (29):

$$dS_t = -\beta_t \xi_t \frac{S_t\left(I_t^A + I_t^M\right)}{N} dt, \quad [4]$$

$$dE_t = \beta_t \xi_t \frac{S_t\left(I_t^A + I_t^M\right)}{N} dt - \nu E_t dt, \quad [5]$$

$$dI_t^A = r\nu E_t dt - p_H \tau_H I_t^A dt - (1-p_H)(1-p_U)\gamma I_t^A dt \quad [6]$$

$$- (1-p_H) p_U \tau_H I_t^A dt, \quad [7]$$

$$dI_t^M = (1-r)\nu E_t dt - \gamma I_t^M dt, \quad [8]$$

$$dH_t = p_H \tau_H I_t^A dt - p_U \tau_U H_t dt - (1-p_U)\tau_F H_t dt, \quad [9]$$

$$dU_t = (1-p_H) p_U \tau_H I_t^A dt + p_U \tau_U H_t dt - \tau_D U_t dt, \quad [10]$$

$$dR_t = \gamma I_t^M dt + \tau_D U_t dt + (1-p_H)(1-p_U)\gamma I_t^A dt \quad [11]$$

$$+ (1-p_U)\tau_F H_t dt, \quad [12]$$

$$dX_t = r\nu\tau_r E_t dt. \quad [13]$$

Here $N$ is the total population size, $X_t$ is the cumulative total of ascertained Ebola cases, $\beta_t$ is the rate of transmission at time $t$, and $\xi_t$ is a lognormal (and hence positive) noise term with mean 1 and variance $\sigma$:

$$\log(\xi_t)\, dt = \sigma dW - \frac{\sigma^2}{2} dt, \quad [14]$$

where $W$ is Brownian motion (29). Model structure and parameters are shown in *SI Appendix*, Fig. S6. The model was simulated using the Euler–Maruyama method with intervals of $dt$=1/10 d. Population size $N$ for each district was taken from Sierra Leone census data (30).

**Model Fitting.** We fitted the model to weekly incidence data (i.e., number of new confirmed and probable cases per week) from Sierra Leone reported in the WHO patient database (1). As described in a previous study, we also used data from the Sierra Leone Ministry of Health (15) when more recent case data were not available in the WHO database (4). We excluded Bonthe district from the analysis as there were small numbers of confirmed or probable cases, which were spaced several weeks apart. It is therefore unlikely there was sustained transmission in this area. For each of the other districts, we used the first reported week of sustained transmission (i.e., there were cases in that week and the following week) as the first data point in the time series. The last data point for all districts was February 2, 2015, as the number of cases had declined to minimal levels in most areas by this point. In the model, incidence in week $t$, denoted $x_t$, was given by the difference in cumulative reported cases over the previous 7 d, i.e., $x_t = X(t) - X(t-7)$. As situation reports were only issued on $w$ out of 7 d in some weeks, we scaled these weeks by a factor $\kappa_t = w/7$. We also included the possibility of variability in the accuracy of reporting in the situation reports. We assumed the number of reported cases in week $t$ followed a negative binomial distribution with mean $x_t\kappa_t$ and variance $\kappa_t x_t + \phi^2 \kappa_t^2 x_t^2$ (4).

Model fitting was performed using a particle Markov chain Monte Carlo (MCMC) algorithm (19) with an adaptive multivariate normal proposal distribution (31). For each district, we fitted the initial number of infective individuals (including both ascertained and missed) at the start of the outbreak, $I_0 = I(0)$; the volatility of the transmission rate, $\sigma$; over-dispersion of reporting, $\phi$; the initial transmission rate $\hat{\beta}$; and the two shape parameters for the transmission rate sigmoid, $a_1$, $a_2$, and $a_\tau$. We used uniform positive priors for all parameters, with the exception of $a_2$, which we constrained to the interval $(-\infty, 1)$ by imposing reflective boundary conditions during parameter resampling. Posterior estimates for $R_0 = \beta_0/\gamma$, $I_0$, $\sigma$, $\phi$, and the 4 sigmoid parameters (taken from 50,000 MCMC iterations, following a burn-in period of 10,000 iterations) are given in *SI Appendix*, Figs. S6–S17; the posterior distribution of the sigmoid is shown in Fig. 2 (blue line and shaded region). The model was implemented in R Version 3.1.3, and parallelized for multiple districts using the doMC library (32, 33).

**Estimating Cases Averted.** To estimate the number of infections averted as a result of control measures, we first estimated the total number of infections (i.e., the cumulative number of individuals who leave the $S$ compartment) up to February 2, 2015 using the posterior parameter estimates from our fitted model. We define this as the "baseline scenario." Next, we assumed that the community transmission rate varied as in the baseline scenario, but no additional EHCs/CCCs/ETUs were introduced. This was equivalent to assuming that changes aside from bed introductions—such as shifts in behavior, increased number of safe burials, improved infection control—would have happened regardless of whether additional beds were made available. We ran 1,000 bootstrap simulations under this scenario, and compared the total number of infections with the baseline scenario. In our main analysis, we assumed that 60% of cases were ascertained (i.e., $r$ = 0.6). To test how sensitive our results were to this assumption, we also refitted the model to each district with $r$ = 0.4 and 0.8, and used these fitted models to estimate the number of cases averted in the two different scenarios above. The results are given in *SI Appendix*, Tables S3 and S4.

**ACKNOWLEDGMENTS.** This work was funded by the Research for Health in Humanitarian Crises (R2HC) Programme, managed by Research for Humanitarian Assistance (Grant 13165). A.J.K. acknowledges support from the Research and Policy for Infectious Disease Dynamics (RAPIDD) program of the Science & Technology Directorate, Department of Homeland Security, and the Fogarty International Center, National Institutes of Health.

1. World Health Organization (2015) Ebola response roadmap situation reports. Available at apps.who.int/ebola/en/current-situation/ebola-situation-report-20-may-2015. Accessed July 1, 2015.
2. Whitty CJ, et al. (2014) Infectious disease: Tough choices to reduce Ebola transmission. *Nature* 515(7526):192–194.
3. World Health Organization (2014) Key considerations for the implementation of Community Care Centres. WHO Report. Available at apps.who.int/iris/bitstream/10665/146469/1/WHO_EVD_Guidance_Strategy_14.3_eng.pdf. Accessed December 10, 2014.
4. Camacho A, et al. (2015) Temporal changes in Ebola transmission in Sierra Leone and implications for control requirements: A real-time modelling study. *PLoS Curr* 7:PMC4339317.
5. Nielsen CF, et al.; Centers for Disease Control and Prevention (2015) Improving burial practices and cemetery management during an Ebola virus disease epidemic - Sierra Leone, 2014. *MMWR Morb Mortal Wkly Rep* 64(1):20–27.
6. Gulland A (2014) UK's plan to build community care centres for Ebola patients is questioned. *BMJ* 349:g6788.
7. BBC News (2015) Ebola crisis: Government response "far too slow." Available at www.bbc.co.uk/news/uk-31366626. Accessed March 15, 2015.
8. Kucharski AJ, et al. (2015) Evaluation of the benefits and risks of introducing Ebola community care centers, Sierra Leone. *Emerg Infect Dis* 21(3):393–399.
9. Lewnard JA, et al. (2014) Dynamics and control of Ebola virus transmission in Montserrado, Liberia: A mathematical modelling analysis. *Lancet Infect Dis* 14(12):1189–1195.
10. Meltzer MI, et al. (2014) Estimating the future number of cases in the Ebola epidemic – Liberia and Sierra Leone, 2014–2015. *MMWR Morb Mortal Wkly Rep* 63(3):1–14.
11. Merler S, et al. (2015) Spatiotemporal spread of the 2014 outbreak of Ebola virus disease in Liberia and the effectiveness of non-pharmaceutical interventions: A computational modelling analysis. *Lancet Infect Dis* 15(2):204–211.
12. Funk S, Knight GM, Jansen VA (2014) Ebola: The power of behaviour change. *Nature* 515(7528):492.
13. The Humanitarian Data Exchange (HDX) (2014) West Africa: Ebola Outbreak. Available at data.hdx.rwlabs.org. Accessed March 27, 2015.
14. Camacho A, et al. (2014) Potential for large outbreaks of Ebola virus disease. *Epidemics* 9:70–78.
15. Sierra Leone Ministry of Health and Sanitation (2014) Ebola virus disease - situation report. Available at health.gov.sl/?page_id=583. Accessed March 20, 2015.
16. WHO Ebola Response Team (2014) Ebola virus disease in West Africa–the first 9 months of the epidemic and forward projections. *N Engl J Med* 371(16):1481–1495.
17. Chowell G, Hengartner NW, Castillo-Chavez C, Fenimore PW, Hyman JM (2004) The basic reproductive number of Ebola and the effects of public health measures: The cases of Congo and Uganda. *J Theor Biol* 229(1):119–126.
18. King AA, Domenech de Cellès M, Magpantay FM, Rohani P (2015) Avoidable errors in the modelling of outbreaks of emerging pathogens, with special reference to Ebola. *Proc Biol Sci* 282(1806):20150347.
19. Andrieu C, Doucet A, Holenstein R (2010) Particle Markov chain Monte Carlo methods. *J R Stat Soc Series B Stat Methodol* 72(3):269–342.
20. Dallatomasina S, et al. (2015) Ebola outbreak in rural West Africa: Epidemiology, clinical features and outcomes. *Trop Med Int Health* 20(4):448–454.
21. Towner JS, et al. (2004) Rapid diagnosis of Ebola hemorrhagic fever by reverse transcription-PCR in an outbreak setting and assessment of patient viral load as a predictor of outcome. *J Virol* 78(8):4330–4341.

22. Hewlett BS, Amola RP (2003) Cultural contexts of Ebola in northern Uganda. *Emerg Infect Dis* 9(10):1242–1248.
23. Ferguson N (2007) Capturing human behaviour. *Nature* 446(7137):733.
24. Funk S, Gilad E, Watkins C, Jansen VA (2009) The spread of awareness and its impact on epidemic outbreaks. *Proc Natl Acad Sci USA* 106(16):6872–6877.
25. Breman J, et al. (1978) The epidemiology of Ebola hemorrhagic fever in Zaire, 1976. *Ebola Virus Haemorrhagic Fever*, ed Pattyn SR (Elsevier, Amsterdam), pp 85–97.
26. Hayden EC (2015) Maternal health: Ebola's lasting legacy. *Nature* 519(7541): 24–26.
27. Takahashi S, et al. (2015) Reduced vaccination and the risk of measles and other childhood infections post-Ebola. *Science* 347(6227):1240–1242.
28. Roberts L (2014) Day 54: Surveillance at odds with justice and the little people. Available at pfmhcolumbia.wordpress.com. Accessed January 5, 2015.
29. Ionides EL, Bretó C, King AA (2006) Inference for nonlinear dynamical systems. *Proc Natl Acad Sci USA* 103(49):18438–18443.
30. National Statistics of Sierra Leone (2004) 2004 population and housing census. Available at www.sierra-leone.org/Census/ssl_final_results.pdf. Accessed April 17, 2015.
31. Roberts GO, Rosenthal JS (2009) Examples of adaptive MCMC. *J Comput Graph Stat* 18:349–367.
32. Revolution Analytics (2014) doMC package. Available at cran.r-project.org/web/packages/doMC/index.html. Accessed March 15, 2015.
33. R Development Core Team (2015) The R Project for Statistical Computing. Available at www.r-project.org/. Accessed March 15, 2015.

# Supplementary materials: Measuring the impact of Ebola control measures in Sierra Leone

Adam J. Kucharski[1], Anton Camacho[1], Stefan Flasche[1], Rebecca E. Glover[1], W. John Edmunds[1], Sebastian Funk[1]

[1] Centre for the Mathematical Modelling of Infectious Diseases, Department of Infectious Disease Epidemiology, London School of Hygiene & Tropical Medicine

## S1 Estimation of duration of infectiousness

The duration of infectiousness, $1/\gamma$, was first calculated separately for cases that result in death and recovery. For cases that resulted in death, the duration of infectiousness was calculated as the reported average duration from onset-to-death (8.6 days) [1] plus one day for burial for cases that were not ascertained (1-$r$) [2]. For cases that recovered, we used the duration from onset-to-hospital discharge (17.2 days) [1] minus 48 hours, as this is the time that would have elapsed since first possible confirmation that the patient was no longer infectious (to be discharged, a patient must test negative for Ebola twice, with an interval of 48 hours between tests [3]). We then combined the two estimates, weighting by the case fatality rate (69%) [1]:

$$1/\gamma = 0.69 \times (8.6 + (1 - r)) + (1 - 0.69) \times (17.2 - 2) \quad \text{(S1)}$$

In our main analysis 60% of cases were ascertained, and hence $1/\gamma$=10.9 days. As a sensitivity analysis we also considered an infectious period of 9 days, equal to the reported average duration from onset-to-death (8.6 days) plus one day for burial for cases that were not ascertained (under 60% ascertainment).

By a similar calculation, the average from onset-to-outcome for cases that seek treatment was $0.69 \times 8.6 + (1 - 0.69) \times (17.2) = 11.3$ days. This value was used to estimate average duration of stay in EHC/CCC/ETU (Table S1).

# References


[1] WHO Ebola Response Team (2014) Ebola virus disease in West Africa — the first 9 months of the epidemic and forward projections. *New England Journal of Medicine* 371:1481–1495.

[2] Nielsen CF, et al. (2015) Improving Burial Practices and Cemetery Management During an Ebola Virus Disease Epidemic. Sierra Leone, 2014. *MMWR. Morbidity and mortality weekly report* 64:20–27.

[3] World Health Organisation (2015) Criteria for declaring the end of the Ebola outbreak in Guinea, Liberia or Sierra Leone. *http://www.who.int/csr/disease/ebola/declaration-ebola-end/en/*.

[4] Breman J, et al. (1978) The epidemiology of Ebola hemorrhagic fever in Zaire, 1976. *Ebola virus haemorrhagic fever (Pattyn, SR ed.)* pp 85–97.

[5] Bentley N (2015) Sierra Leone Ebola labs project – beating the outbreak at source. *Public Health England Blog*.

[6] World Health Organisation (2015) Ebola response roadmap situation reports. *apps.who.int/ebola/en/current-situation/ebola-situation-report-20-may-2015*.

# Supplementary Tables

Table S1: Parameter definitions and values.

| Parameter | Definition | Value | Reference |
|---|---|---|---|
| $1/\nu$ | Latent period | 9.4 days | [1, 4] |
| $1/\gamma$ | Mean duration of infectiousness | 10.9 days | See supplementary text |
| $1/\tau_H$ | Mean time from onset of symptoms to EHC/CCC admission | 1.8 to 4.6 days | See Fig. S1 |
| $1/\tau_U$ | Mean time spent in EHC/CCC awaiting test results | 2 days | [5] |
| $1/\tau_D$ | Mean duration of stay in ETU | $11.3-1/\tau_H - 1/\tau_U$ | |
| $1/\tau_F$ | Mean duration of stay in EHC/CCC if no ETU beds | $11.3-1/\tau_H$ | |
| $1/\nu$ | Mean time from onset of symptoms to case report | 4.5 days | [1] |
| $r$ | Proportion of cases that are ascertained | 0.4, 0.6, 0.8 | |
| $\hat{\beta}$ | Initial transmission rate | Estimated | |
| $a_1$ | Slope of change in transmission rate | Estimated | |
| $a_2$ | Final value of transmission rate | Estimated | |
| $a_\tau$ | Midpoint of time of change in transmission rate | Estimated | |
| $\sigma$ | Volatility of transmission rate | Estimated | |
| $\phi$ | Overdispersion of reporting process | Estimated | |

Table S2: Relationship between relative reduction in $R_0$, initial $R_0$, and total cases per 100,000 population in each district. Relative reduction in $R_0$ is calculated as $1 - R_0^T/R_0^0$, where $R_0^0$ is the median basic reproduction number at the start of the period of study, and $R_0^T$ is the median basic reproduction number on 2nd February 2015. Association between reduction and the other two variables was tested using Pearson's product moment correlation coefficient.

| District | Relative reduction in $R_0$ | Initial $R_0$ | Cases/100,000 |
|---|---|---|---|
| Pujehun | -8.74E-11 | 0.546 | 12.7 |
| Koinadugu | -2.52E-15 | 0.792 | 62.1 |
| Bo | 1.52E-08 | 1.76 | 89.7 |
| Kambia | 0.000795 | 1.98 | 69.1 |
| Tonkolili | 0.00158 | 1.31 | 179 |
| Moyamba | 0.00281 | 1.1 | 107 |
| Port Loko | 0.0661 | 1.55 | 437 |
| Kono | 0.148 | 1.81 | 151 |
| Kenema | 0.299 | 2.39 | 114 |
| Western Area | 0.378 | 2.41 | 395 |
| Bombali | 0.553 | 3.36 | 264 |
| Kailahun | 0.604 | 3.31 | 206 |
| | Correlation: | 0.905 | 0.445 |
| | p-value: | $<$0.0001 | 0.147 |

Table S3: Estimated number of cases averted up to 2nd February 2015 as a result of additional treatment beds, when $1/\gamma$=10.9 days and 80% cases are ascertained.

| District | Initial $R_0$ | Beds introduced | Additional beds | Beds 4 weeks earlier |
|---|---|---|---|---|
| Bo | 1.8 (1.6–2.3) | 124 | 14,600 (388–39,000) | 15,100 (423–89,700) |
| Bombali | 3.4 (2.2–5.2) | 506 | 8,570 (4–73,400) | 12,500 (2–207,000) |
| Kailahun | 3.3 (2.9–3.8) | 123 | 20,500 (12,200–36,900) | 21,400 (13,200–37,700) |
| Kambia | 2.0 (1.4–9.6) | 55 | 532 (0–4,970) | 679 (0–20,000) |
| Kenema | 2.4 (1.7–4.0) | 75 | 274 (199–411) | 440 (304–635) |
| Koinadugu | 0.8 (0.6–1.2) | 92 | 62 (26–189) | 144 (79–290) |
| Kono | 1.8 (1.5–16.2) | 83 | 1,730 (0–3,580) | 2,440 (0–7,810) |
| Moyamba | 1.1 (0.9–5.4) | 34 | 138 (72–253) | 243 (153–442) |
| Port Loko | 1.6 (1.5–1.7) | 546 | 8,410 (5,680–11,600) | 10,300 (7,160–14,200) |
| Pujehun | 0.5 (0.4–1.0) | 24 | 12 (5–41) | 25 (12–58) |
| Tonkolili | 1.3 (1.1–2.8) | 349 | 1,300 (10–8,470) | 1,680 (18–12,000) |
| Western Area | 2.4 (2.3–2.6) | 960 | 82,800 (67,100–109,000) | 89,200 (73,300–114,000) |
| Total | | 2971 | 148,000 (115,000–219,000) | 159,000 (126,000–351,000) |

Table S4: Estimated number of cases averted up to 2nd February 2015 as a result of reduction in community transmission and/or additional treatment beds, when $1/\gamma$=10.9 days and 40% cases are ascertained.

| District | Initial $R_0$ | Beds introduced | Additional beds | Beds 4 weeks earlier |
|---|---|---|---|---|
| Bo | 1.9 (1.4–3.2) | 124 | 2,150 (1,140–4,670) | 2,770 (1,430–8,580) |
| Bombali | 4.1 (3.3–5.7) | 506 | 3,460 (2,960–4,270) | 4,600 (4,000–5,570) |
| Kailahun | 6.2 (1.7–11.5) | 123 | 1,420 (0–9,520) | 2,430 (1–22,800) |
| Kambia | 1.4 (1.2–1.5) | 55 | 432 (295–578) | 641 (446–816) |
| Kenema | 2.2 (1–14.7) | 75 | 120 (0–12,700) | 181 (0–18,400) |
| Koinadugu | 0.6 (0.3–0.9) | 92 | 29 (12–96) | 95 (51–208) |
| Kono | 3.5 (1.3–19.3) | 83 | 78 (0–3,020) | 132 (0–8,600) |
| Moyamba | 1.1 (0.8–12.2) | 34 | 97 (0–549) | 187 (0–1,340) |
| Port Loko | 2.3 (1.8–3.0) | 546 | 2,450 (369–6,980) | 4,230 (629–12,600) |
| Pujehun | 0.5 (0.3–1.4) | 24 | 9 (2–28) | 23 (9–51) |
| Tonkolili | 2.9 (1.7–6.6) | 349 | 400 (133–850) | 788 (292–1,660) |
| Western Area | 2.5 (2.3–2.9) | 960 | 17,600 (14,600–20,900) | 25,000 (19,800–28,700) |
| Total | | 2971 | 29,200 (24,500–47,700) | 42,600 (34,700–75,000) |

Table S5: Estimated number of cases averted up to 2nd February 2015 as a result of additional treatment beds, when $1/\gamma$=9 days and 60% cases are ascertained.

| District | Initial $R_0$ | Beds introduced | Additional beds | Beds 4 weeks earlier |
|---|---|---|---|---|
| Bo | 1.6 (1.4–2) | 124 | 5,170 (2,710–8,920) | 5,700 (3,270–9,460) |
| Bombali | 5.7 (3.8–8.2) | 506 | 5,640 (4,720–6,900) | 6,720 (5,800–7,940) |
| Kailahun | 6 (4.1–14.8) | 123 | 3,550 (1,830–5,880) | 4,330 (2,940–6,770) |
| Kambia | 1.5 (1.2–3) | 55 | 547 (89–2,570) | 745 (132–6,900) |
| Kenema | 3.5 (1.4–14.4) | 75 | 0 (0–31,300) | 1 (0–47,700) |
| Koinadugu | 0.7 (0.4–2.3) | 92 | 31 (9–121) | 95 (42–222) |
| Kono | 1.6 (1.4–12) | 83 | 1,180 (0–4,220) | 1,640 (0–12,700) |
| Moyamba | 1.1 (0.7–6.6) | 34 | 121 (0–1,380) | 224 (0–2,590) |
| Port Loko | 1.7 (1.4–2) | 546 | 3,960 (3,250–5,080) | 5,760 (4,960–7,120) |
| Pujehun | 0.6 (0.3–0.8) | 24 | 10 (2–27) | 21 (8–47) |
| Tonkolili | 2.8 (1.4–6.8) | 349 | 571 (370–846) | 956 (689–1,290) |
| Western Area | 2.3 (2.1–2.6) | 960 | 33,100 (26,200–41,200) | 39,500 (32,500–47,200) |
| Total | | 2971 | 54,800 (45,400–79,100) | 67,500 (58,500–118,000) |

Table S6: Estimated number of cases averted up to 2nd February 2015 as a result of additional treatment beds, when districts have additional imported cases. These extra cases are added to the $I_t^A$ and $I_t^N$ compartments in the model (weighted by the ascertainment rate, $r$) at an average rate of either one per day or one per week. We assume $1/\gamma$=10.9 days and 60% cases are ascertained.

| District | Initial $R_0$ | Beds introduced | With one imported case per day | With one imported case per week |
|---|---|---|---|---|
| Bo | 1.6 (1.4–1.7) | 124 | 8,450 (5,600–13,100) | 6,680 (4,320–10,500) |
| Bombali | 5.2 (2.9–7.9) | 506 | 14,300 (3,850–18,400) | 10,500 (1,090–16,100) |
| Kailahun | 8.4 (5.3–16.2) | 123 | 5,070 (2,900–9,190) | 3,960 (2,190–7,090) |
| Kambia | 1.5 (1.4–3.6) | 55 | 936 (13–3,260) | 612 (13–4,180) |
| Kenema | 7.4 (2.1–19.4) | 75 | 2 (0–12,700) | 1 (0–16,200) |
| Koinadugu | 0.7 (0.3–1.1) | 92 | 49 (19–170) | 39 (14–114) |
| Kono | 1.6 (1.4–1.9) | 83 | 1,930 (1,030–2,980) | 1,610 (941–2,480) |
| Moyamba | 1 (0.9–1.2) | 34 | 145 (89–231) | 125 (77–205) |
| Port Loko | 1.8 (1.6–2.2) | 546 | 4,210 (1,280–9,380) | 3,900 (1,060–15,300) |
| Pujehun | 0.5 (0.2–1.2) | 24 | 19 (3–46) | 11 (3–43) |
| Tonkolili | 3.5 (1.3–8.4) | 349 | 780 (61–2,710) | 601 (28–4,610) |
| Western Area | 2.5 (2.2–2.8) | 960 | 35,600 (27,600–46,500) | 33,100 (25,300–42,300) |
| Total | | 2971 | 72,900 (61,700–87,900) | 64,900 (49,800–93,100) |

# Supplementary Figures

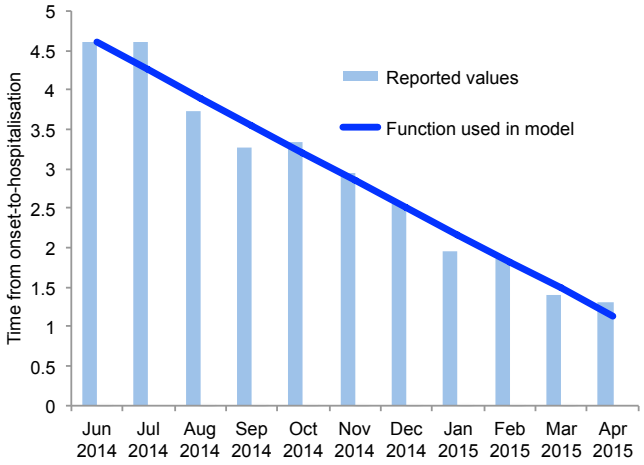


Figure S1: Decline in time from onset-to-isolation. We assume the delay in June and July 2014 was equal to the average value reported in an early summary analysis [1]; the remaining values come from WHO situation reports [6]. We used linear regression to obtain the continuos-time function used in the model.

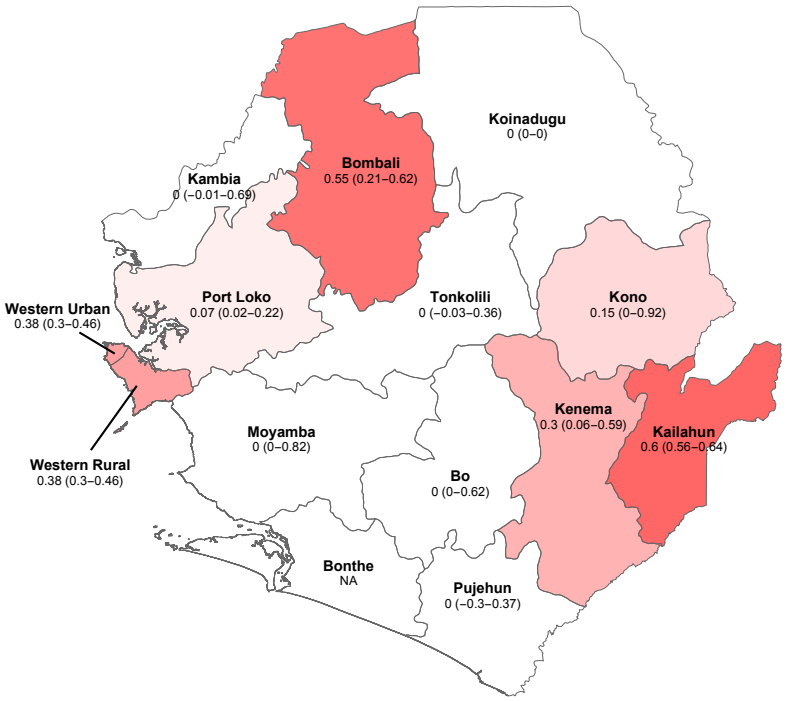


Figure S2: Relative reduction in $R_0$ in different districts. This is calculated as $1 - R_0^T / R_0^0$, where $R_0^0$ is the basic reproduction number at the start of the period of study, and $R_0^T$ is the basic reproduction number on 2nd February 2015. Districts are coloured by median reduction in $R_0$, the value for which is given below the district name (95% credible intervals are in parentheses). In the model we treated the two parts of Western Area (Urban and Rural) as one district, as this is how case data were typically reported. There was no estimate of reduction in Bonthe, as we did not fit the model to this district (see main text for details). District boundaries obtained from the GADM database of Global Administrative Areas, freely available from *http://www.gadm.org* .

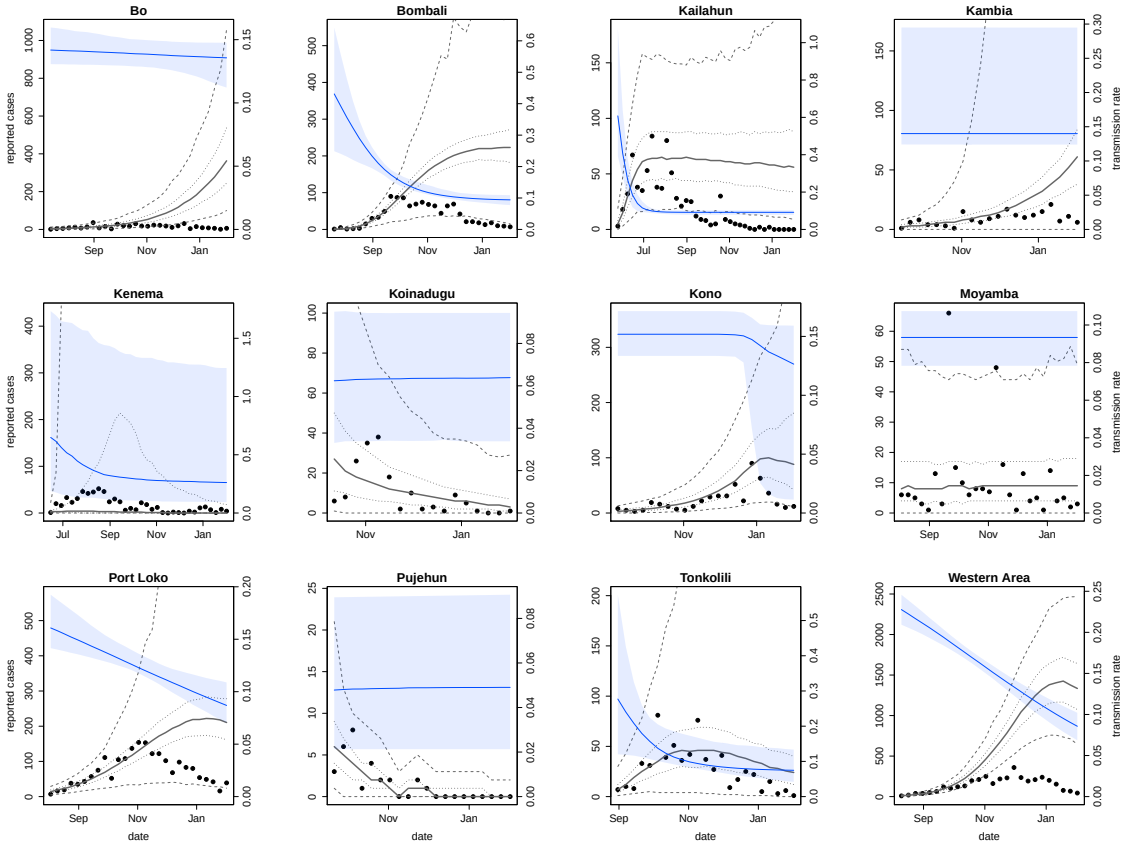


Figure S3: District-level epidemic dynamics in the absence of treatment beds. Gray line shows median number of cases generated from 1000 simulations of the fitted model, with 50% credible intervals given by dotted gray lines and 95% CI given by dashed lines. Blue line shows median community transmission rate, shaded area shows 95% credible interval (right hand axis). Black dots show weekly reported confirmed and probable cases in each district up to 2nd February 2015 (left hand axis).

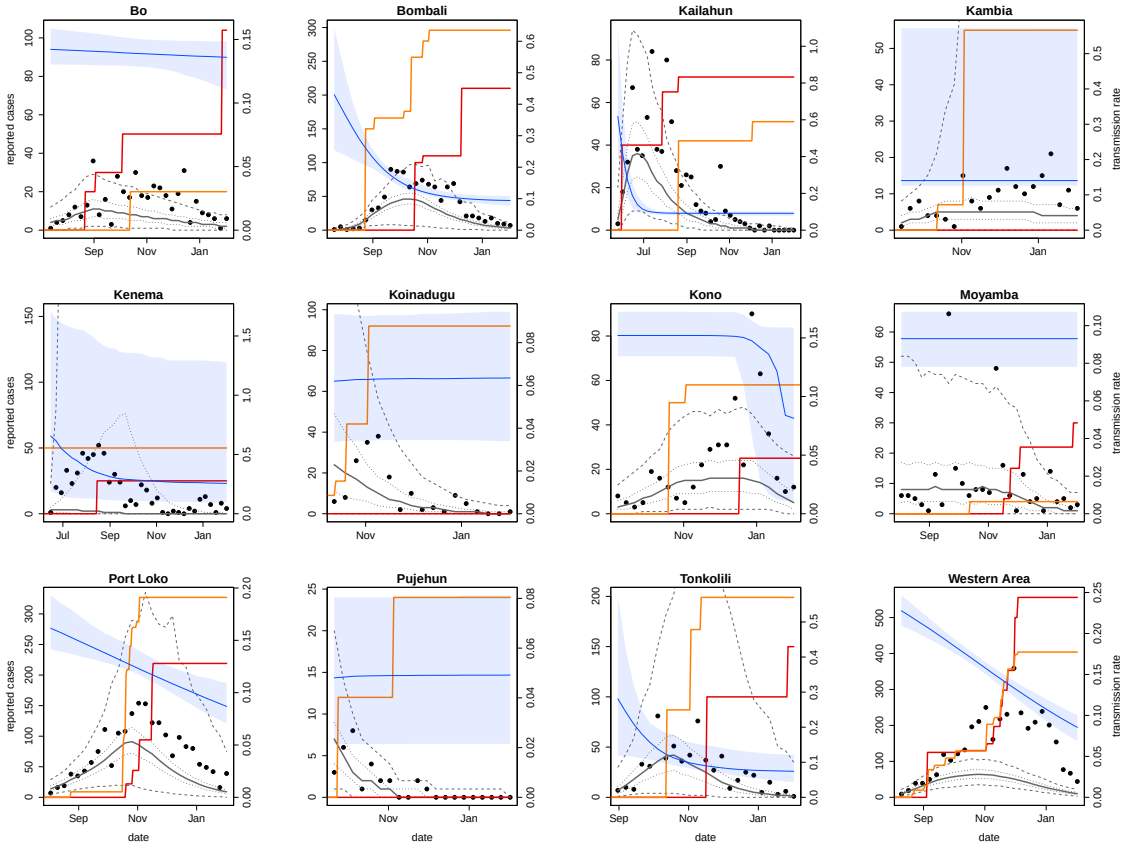


Figure S4: District-level epidemic dynamics when beds are introduced 4 weeks earlier. Gray line shows median number of cases generated from 1000 simulations of the fitted model, with 50% credible intervals given by dotted gray lines and 95% CI given by dashed lines. Blue line shows median community transmission rate, shaded area shows 95% credible interval (right hand axis). Black dots show weekly reported confirmed and probable cases in each district up to 2nd February 2015 (left hand axis). Solid red line, ETU bed capacity; orange line, EHC/CCC bed capacity.

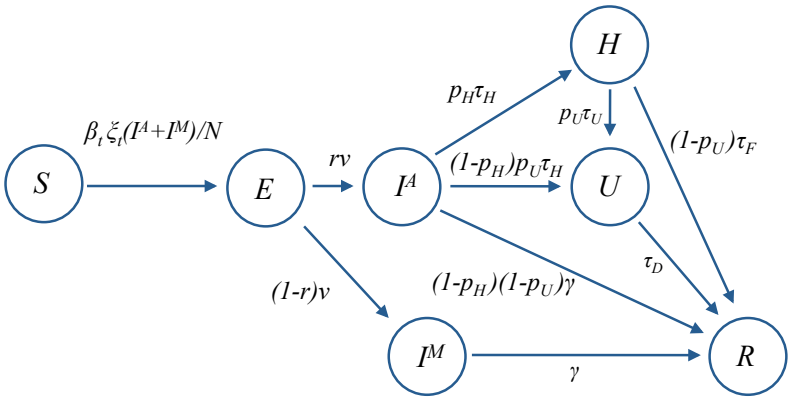


Figure S5: Model structure. Individuals start off susceptible to infection ($S$). Upon infection with Ebola they enter an incubation period ($E$), then at symptom onset they become infectious; these individuals either eventually become ascertained ($I^A$) or do not ($I^M$). Individuals who are ascertained initially seek health care in EHC/CCCs (or ETUs if these are full); if no beds are available, they remain infectious in the community until the infection is resolved ($R$) i.e. they have recovered, or are dead and buried. Patients in EHC/CCCs are transferred to ETUs once they have been tested for Ebola, which takes an average of 2 days. Patients remain in ETUs until the infection is resolved. We assume the latent period is 9.4 days, the average time from onset to EHC/CCC attendance is 4.6 days, and individuals who do not seek treatment are infectious for 11.3 days on average[1].

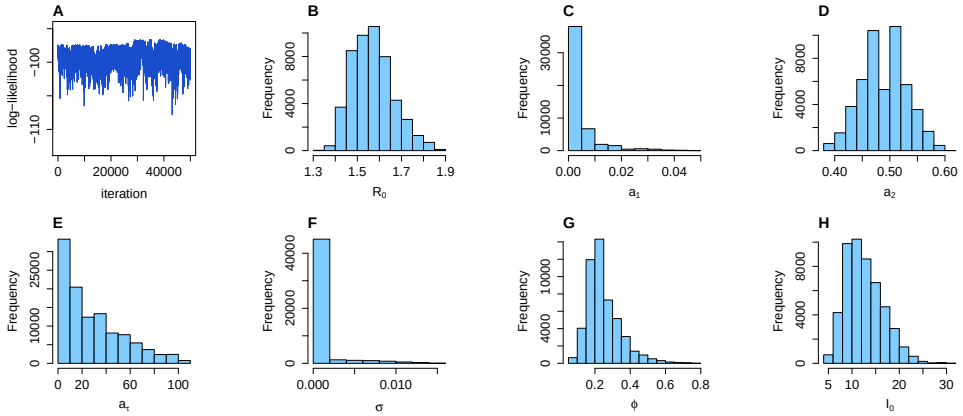


Figure S6: Estimated posterior parameter distributions for Bo. (A) MCMC trace plot of log-likelihood. (B) Basic reproduction number at the start of the outbreak in the district, $R_0 = \beta_0/\gamma$. (C) Slope of the time-varying transmission rate sigmoid, $a_1$. (D) Final value of sigmoid, $a_2$. (E) Midpoint of sigmoid, $a_\tau$. (F) Volatility of transmission noise, $\sigma$. (G) Reporting error, $\phi$. (H) Initial number of infectious individuals, $I_0$.

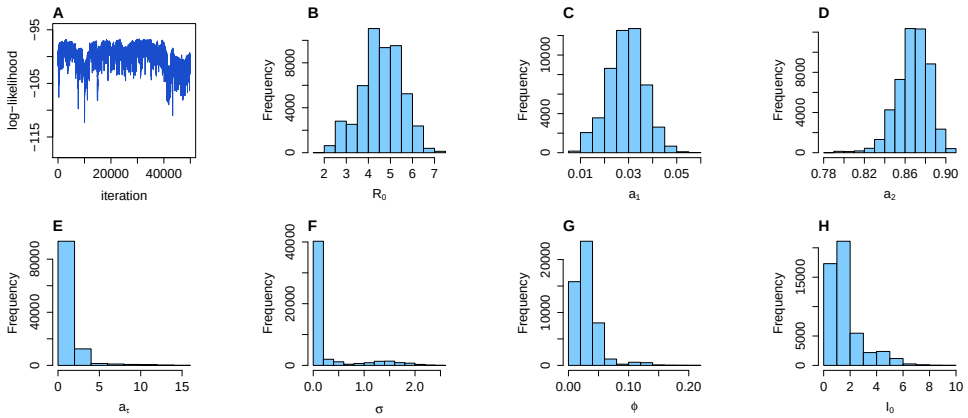


Figure S7: Estimated posterior parameter distributions for Bombali. (A) MCMC trace plot of log-likelihood. (B) Basic reproduction number at the start of the outbreak in the district, $R_0 = \beta_0/\gamma$. (C) Slope of the time-varying transmission rate sigmoid, $a_1$. (D) Final value of sigmoid, $a_2$. (E) Midpoint of sigmoid, $a_\tau$. (F) Volatility of transmission noise, $\sigma$. (G) Reporting error, $\phi$. (H) Initial number of infectious individuals, $I_0$.

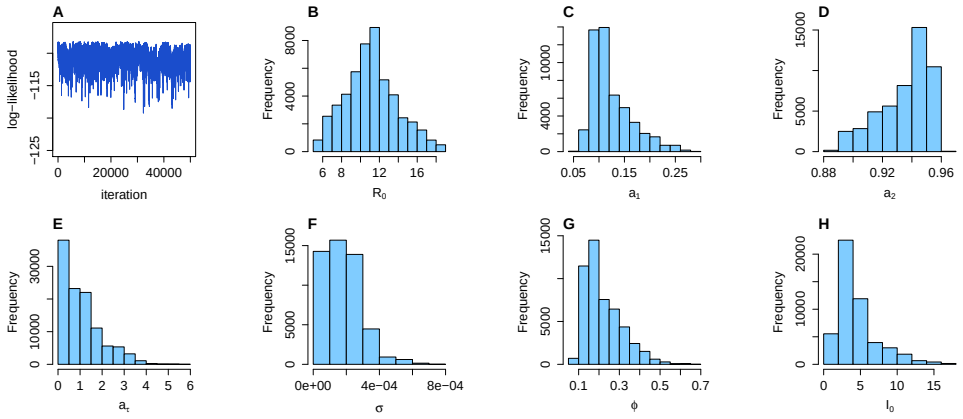


Figure S8: Estimated posterior parameter distributions for Kailahun. (A) MCMC trace plot of log-likelihood. (B) Basic reproduction number at the start of the outbreak in the district, $R_0 = \beta_0/\gamma$. (C) Slope of the time-varying transmission rate sigmoid, $a_1$. (D) Final value of sigmoid, $a_2$. (E) Midpoint of sigmoid, $a_\tau$. (F) Volatility of transmission noise, $\sigma$. (G) Reporting error, $\phi$. (H) Initial number of infectious individuals, $I_0$.

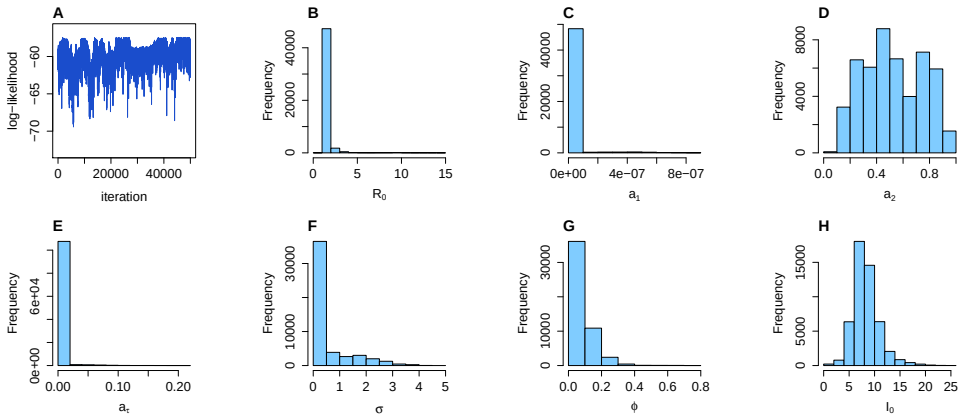


Figure S9: Estimated posterior parameter distributions for Kambia. (A) MCMC trace plot of log-likelihood. (B) Basic reproduction number at the start of the outbreak in the district, $R_0 = \beta_0/\gamma$. (C) Slope of the time-varying transmission rate sigmoid, $a_1$. (D) Final value of sigmoid, $a_2$. (E) Midpoint of sigmoid, $a_\tau$. (F) Volatility of transmission noise, $\sigma$. (G) Reporting error, $\phi$. (H) Initial number of infectious individuals, $I_0$.

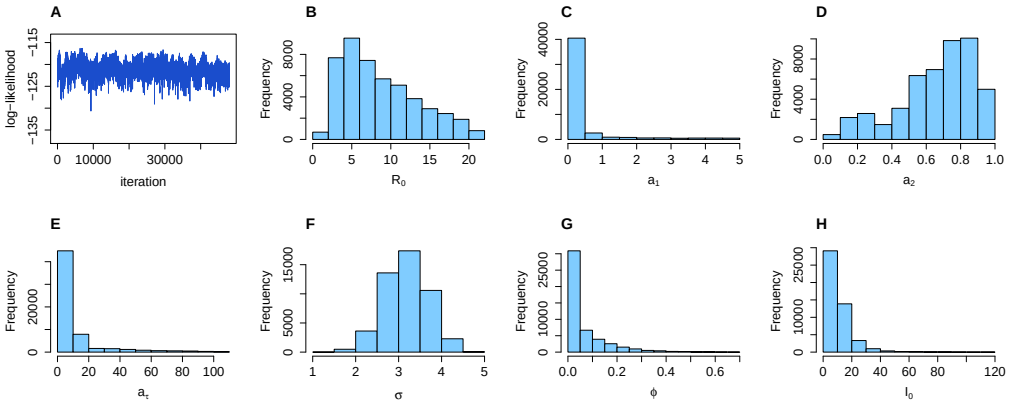


Figure S10: Estimated posterior parameter distributions for Kenema. (A) MCMC trace plot of log-likelihood. (B) Basic reproduction number at the start of the outbreak in the district, $R_0 = \beta_0/\gamma$. (C) Slope of the time-varying transmission rate sigmoid, $a_1$. (D) Final value of sigmoid, $a_2$. (E) Midpoint of sigmoid, $a_\tau$. (F) Volatility of transmission noise, $\sigma$. (G) Reporting error, $\phi$. (H) Initial number of infectious individuals, $I_0$.

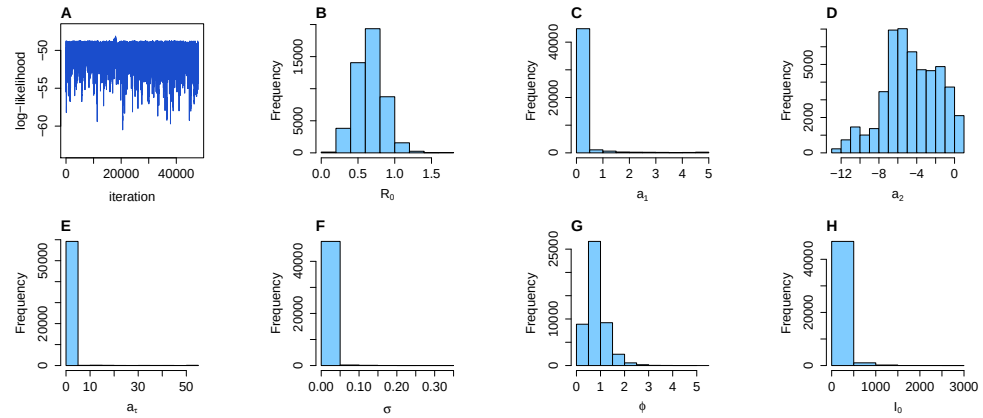


Figure S11: Estimated posterior parameter distributions for Koinadugu. (A) MCMC trace plot of log-likelihood. (B) Basic reproduction number at the start of the outbreak in the district, $R_0 = \beta_0/\gamma$. (C) Slope of the time-varying transmission rate sigmoid, $a_1$. (D) Final value of sigmoid, $a_2$. (E) Midpoint of sigmoid, $a_\tau$. (F) Volatility of transmission noise, $\sigma$. (G) Reporting error, $\phi$. (H) Initial number of infectious individuals, $I_0$.

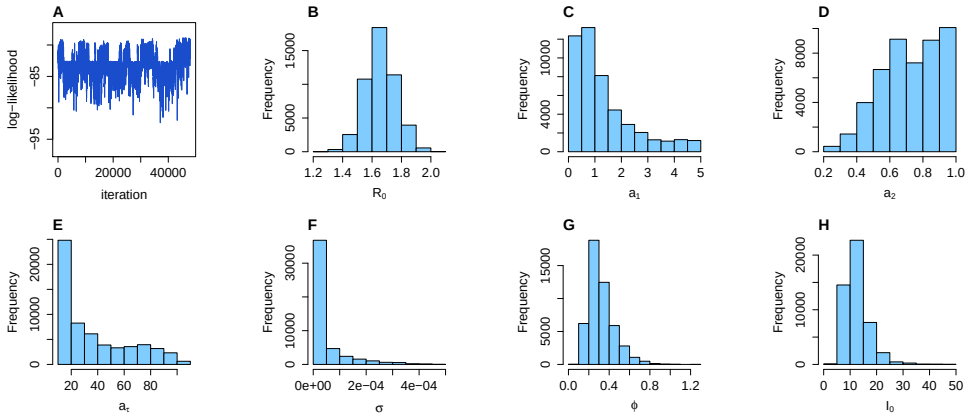


Figure S12: Estimated posterior parameter distributions for Kono. (A) MCMC trace plot of log-likelihood. (B) Basic reproduction number at the start of the outbreak in the district, $R_0 = \beta_0/\gamma$. (C) Slope of the time-varying transmission rate sigmoid, $a_1$. (D) Final value of sigmoid, $a_2$. (E) Midpoint of sigmoid, $a_\tau$. (F) Volatility of transmission noise, $\sigma$. (G) Reporting error, $\phi$. (H) Initial number of infectious individuals, $I_0$.The bimodal distribution of the log-likelihood is the result of the two peaks in epidemic time series; the model switches between these peaks when fitting the sigmoid, which leads to the broad posterior distribution for $a_\tau$.

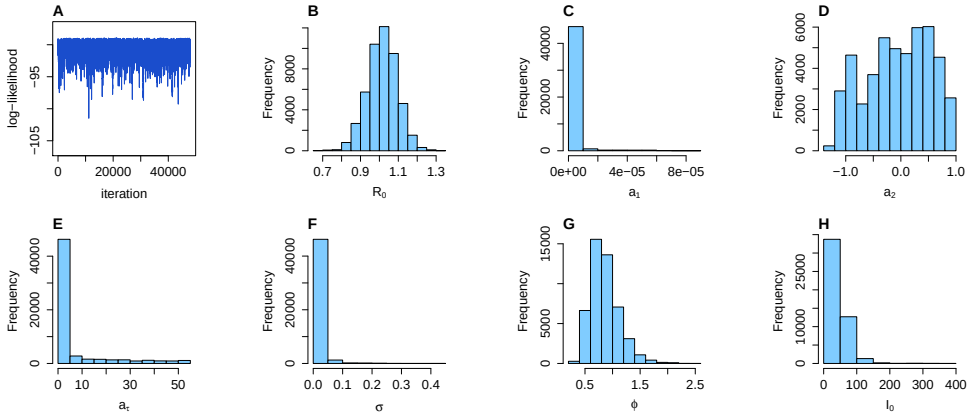


Figure S13: Estimated posterior parameter distributions for Moyamba. (A) MCMC trace plot of log-likelihood. (B) Basic reproduction number at the start of the outbreak in the district, $R_0 = \beta_0/\gamma$. (C) Slope of the time-varying transmission rate sigmoid, $a_1$. (D) Final value of sigmoid, $a_2$. (E) Midpoint of sigmoid, $a_\tau$. (F) Volatility of transmission noise, $\sigma$. (G) Reporting error, $\phi$. (H) Initial number of infectious individuals, $I_0$.

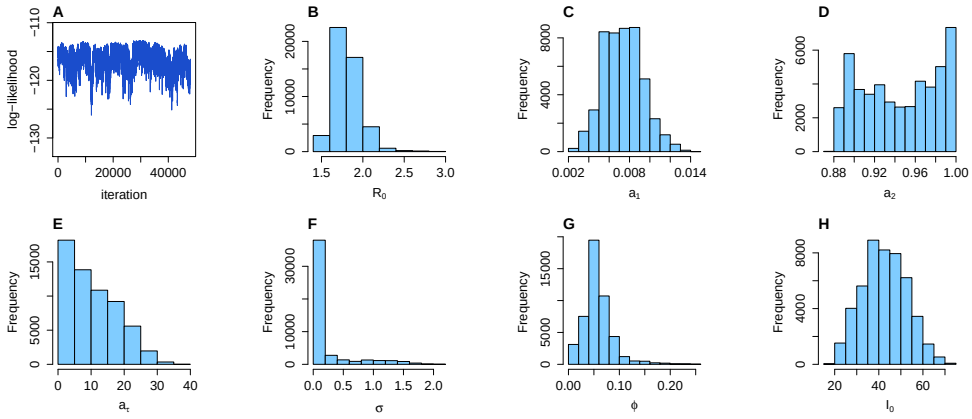


Figure S14: Estimated posterior parameter distributions for Port Loko. (A) MCMC trace plot of log-likelihood. (B) Basic reproduction number at the start of the outbreak in the district, $R_0 = \beta_0/\gamma$. (C) Slope of the time-varying transmission rate sigmoid, $a_1$. (D) Final value of sigmoid, $a_2$. (E) Midpoint of sigmoid, $a_\tau$. (F) Volatility of transmission noise, $\sigma$. (G) Reporting error, $\phi$. (H) Initial number of infectious individuals, $I_0$.

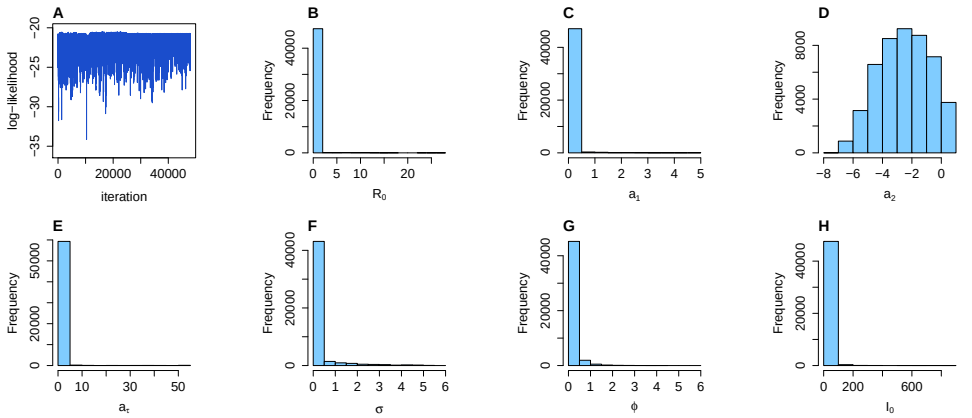


Figure S15: Estimated posterior parameter distributions for Pujehun. (A) MCMC trace plot of log-likelihood. (B) Basic reproduction number at the start of the outbreak in the district, $R_0 = \beta_0/\gamma$. (C) Slope of the time-varying transmission rate sigmoid, $a_1$. (D) Final value of sigmoid, $a_2$. (E) Midpoint of sigmoid, $a_\tau$. (F) Volatility of transmission noise, $\sigma$. (G) Reporting error, $\phi$. (H) Initial number of infectious individuals, $I_0$.

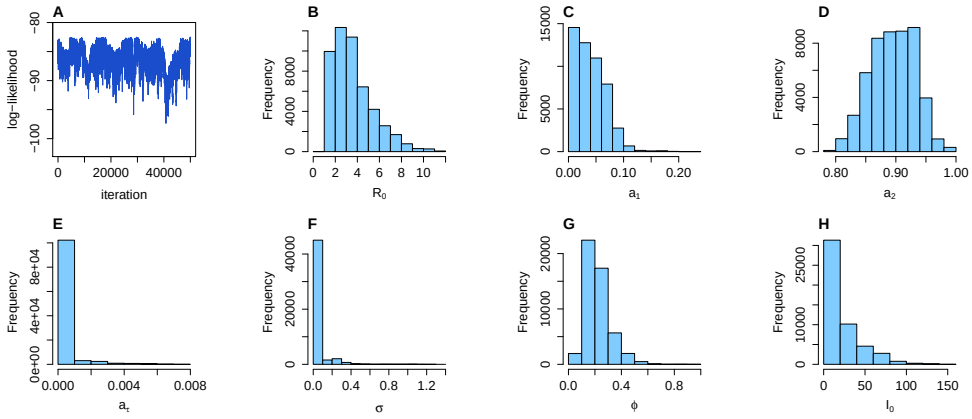


Figure S16: Estimated posterior parameter distributions for Tonkolili. (A) MCMC trace plot of log-likelihood. (B) Basic reproduction number at the start of the outbreak in the district, $R_0 = \beta_0/\gamma$. (C) Slope of the time-varying transmission rate sigmoid, $a_1$. (D) Final value of sigmoid, $a_2$. (E) Midpoint of sigmoid, $a_\tau$. (F) Volatility of transmission noise, $\sigma$. (G) Reporting error, $\phi$. (H) Initial number of infectious individuals, $I_0$.

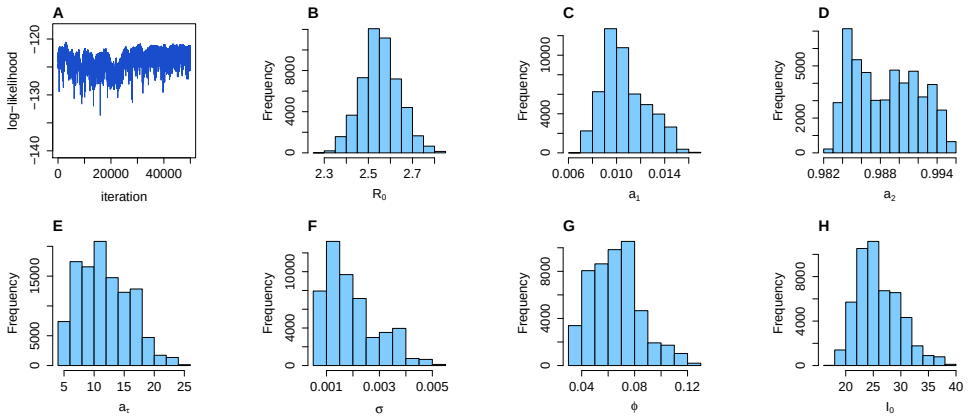


Figure S17: Estimated posterior parameter distributions for Western Area. (A) MCMC trace plot of log-likelihood. (B) Basic reproduction number at the start of the outbreak in the district, $R_0 = \beta_0/\gamma$. (C) Slope of the time-varying transmission rate sigmoid, $a_1$. (D) Final value of sigmoid, $a_2$. (E) Midpoint of sigmoid, $a_\tau$. (F) Volatility of transmission noise, $\sigma$. (G) Reporting error, $\phi$. (H) Initial number of infectious individuals, $I_0$.